

Energy transfer in *Anabaena variabilis* filaments under nitrogen depletion, studied by time-resolved fluorescence

Aya Onishi · Shimpei Aikawa · Akihiko Kondo ·
Seiji Akimoto

Received: 26 September 2014 / Accepted: 12 January 2015 / Published online: 18 January 2015
© Springer Science+Business Media Dordrecht 2015

Abstract Some filamentous cyanobacteria (including *Anabaena*) differentiate into heterocysts under nitrogen-depleted conditions. During differentiation, the phycobili-proteins and photosystem II in the heterocysts are gradually degraded. Nitrogen depletion induces changes in the pigment composition of both vegetative cells and heterocysts, which affect the excitation energy transfer processes. To investigate the changes in excitation energy transfer processes of *Anabaena variabilis* filaments grown in standard medium (BG11) and a nitrogen-free medium (BG11₀), we measured their steady-state absorption spectra, steady-state fluorescence spectra, and time-resolved fluorescence spectra (TRFS) at 77 K. TRFS were measured with a picosecond time-correlated single photon counting system. The pigment compositions of the filaments grown in BG11₀ changed throughout the growth period; the relative phycocyanin levels monotonically decreased, whereas the relative carotenoid (Car) levels decreased and then recovered to their initial value (at day 0), with formation of lower-energy Cars. Nitrogen starvation also altered the

fluorescence kinetics of PSI; the fluorescence maximum of TRFS immediately after excitation occurred at 735, 740, and 730 nm after 4, 8, and 15 days growth in BG11₀, respectively. Based on these results, we discuss the excitation energy transfer dynamics of *A. variabilis* filaments under the nitrogen-depleted condition throughout the growth period.

Keywords Energy transfer · Time-resolved fluorescence · Nitrogen depletion · Cyanobacteria

Abbreviations

APC	Allophycocyanin
Car	Carotenoid
Chl	Chlorophyll
FDAS	Fluorescence decay-associated spectra
PBS	Phycobilisome
PC	Phycocyanin
PEC	Phycoerythrocyanin
PS	Photosystem
TRFS	Time-resolved fluorescence spectra

A. Onishi · S. Akimoto
Graduate School of Science, Kobe University, Kobe 657-8501,
Japan

S. Aikawa · A. Kondo
Graduate School of Engineering, Kobe University,
Kobe 657-8501, Japan

S. Aikawa · A. Kondo · S. Akimoto
Japan Science and Technology Agency, CREST,
Kobe 657-8501, Japan

S. Akimoto (✉)
Molecular Photoscience Research Center, Kobe University,
Kobe 657-8501, Japan
e-mail: akimoto@hawk.kobe-u.ac.jp

Introduction

Photosynthetic organisms respond to changes in light, nutrient, and other environmental conditions by regulating their primary photosynthetic processes. Pigment compositions alter under different light colors and intensities (Ghosh and Govindjee 1966). Under high-light conditions, photosynthetic organisms regulate their antenna complexes (Owens 1996) and dissipate the excess excitation energy to prevent severe photodamage caused by the highly reactive

excited singlet state of oxygen (Melis 1999; Takahashi and Badger 2011). Energy transfer processes depend on the quality and intensity of the light, and on the growth period (Akimoto et al. 2013). Nutritional deficiency also induces modifications in various photosynthetic organisms. Inorganic nutrients such as nitrogen, sulfur, and phosphorus are particularly important for most cyanobacteria and many other photosynthetic organisms. When cyanobacteria are grown in conditions lacking these essential inorganic elements, their phycobilisomes (PBSs) are degraded (Allen and Smith 1969; Jensen and Rachlin 1984) and their growth is compromised (Collier et al. 1994). Nitrogen is especially important because it is incorporated into the proteins and nucleic acids of photosynthetic organisms, and is used in photosynthesis and other biological activities. Allen and Smith (1969) reported that *Synechococcus elongatus* (*Anacystis nidulans*) grown in low-nitrate medium (NaNO_3 level 1/40 that of complete growth medium) increases its carotenoids (Cars) content relative to chlorophyll (Chl). However, the relative intensities of Chl and Car in the absorption spectrum of *Arthrospira* (*Spirulina*) *platensis* grown in low-nitrogen medium (NaNO_3 level 1/10 that of complete growth medium) were unaltered. This suggests that the nutrient stress in the second study was insufficient to affect the Chl and Car levels (Peter et al. 2010).

Molecular nitrogen is abundant in Earth's atmosphere but is inaccessible to photosynthetic organisms because it is unreactive. Therefore, atmospheric molecular nitrogen must be converted into reactive forms such as ionic ammonium, nitrite, and nitrate. Under nitrogen-depleted conditions, cyanobacteria unable to fix nitrogen become bleached, and alter from blue–green to yellow as their pigment compositions alter (Lau et al. 1977). On the other hand, *Anabaena* and some other filamentous cyanobacteria can grow diazotrophically, and can therefore adapt to nitrogen-limited conditions. In these organisms, some of the vegetative cells differentiate into specialized cells called heterocysts that self-source their nitrogen requirements. Heterocysts fix atmospheric molecular nitrogen by producing a nitrogen-fixing enzyme, nitrogenase. The fixed nitrogen is transferred from heterocysts to nearby vegetative cells as amino acid in the nitrogen-fixing filaments; in return, the heterocysts receive fixed carbon from the vegetative cells (Golden and Yoon 2003). Heterocyst differentiation is triggered by nitrogen deprivation. Approximately, 5–10 % of *A. variabilis* cells grown in nitrogen-free medium are heterocysts (Haselkorn 1978), and mature heterocysts are formed within 18–24 h of nitrogen source removal (Flores and Herrero 2010).

The PBS of *A. variabilis* contains three types of phycobiliproteins (PBPs): allophycocyanin (APC), phycocyanin (PC), and phycoerythrocyanin (PEC). The PBS is

hemidiscoidally shaped; APC is contained in its core complex, whereas PC and PEC reside in its rods (Zhao et al. 1999; Watanabe and Ikeuchi 2013). During heterocyst differentiation, photosystem (PS) II and PBPs are gradually degraded. Depletion of a nitrogen source also initiates PBP degradation in vegetative cells, which continues until the cells receive sufficient nitrogen compounds from the heterocysts. Previous spectroscopic studies on heterocyst differentiation in *A. variabilis* have considered PBS and PSII degradation during this period, or whether levels of PSI are altered. PSII is known to be degraded along with APC in heterocysts, but small amounts of PEC and PC remain (Kumazaki et al. 2013). In contrast, intercellular PSI levels are unaltered under nitrogen-depleted conditions because PSI is essential for ATP production, by which nitrogen fixation proceeds (Sugiura and Itoh 2012; Kumazaki et al. 2013). *A. variabilis* also contains PSI tetramers and a PSI-specific antenna, which may play a role in light harvesting and promoting nitrogen fixation (Watanabe et al. 2014).

Whereas the degradation of PBPs and PSII under nitrogen stress and during heterocyst differentiation has been well documented, the changes in the excitation energy transfer processes of *A. variabilis* filaments remain unclear. These changes in photosynthetic organisms can be properly monitored by time-resolved fluorescence spectroscopy, which detects signals only from pigments in excited states. Therefore, we can investigate the excitation energy transfer processes at different times after excitation. Here, we discuss the in vivo energy transfer processes of *A. variabilis* filaments under nitrogen-depleted conditions by measuring and analyzing the steady-state absorption and fluorescence spectra and time-resolved fluorescence spectra.

Materials and methods

Culture conditions

Anabaena variabilis ATCC 29413 filaments were pre-cultured in 200 mL Erlenmeyer flasks containing 70 mL of modified BG11 medium [NaNO_3 (1.5 g L^{-1}), K_2HPO_4 (0.04 g L^{-1}), $\text{MgSO}_4 \cdot \text{H}_2\text{O}$ (0.075 g L^{-1}), $\text{CaCl}_2 \cdot 2\text{H}_2\text{O}$ (0.036 g L^{-1}), citric acid (0.006 g L^{-1}), ferric citrate (0.006 g L^{-1}), EDTA (disodium salt; 0.001 g L^{-1}), Na_2CO_3 (0.02 g L^{-1}), H_3BO_3 (2.86 mg L^{-1}), $\text{MnCl}_2 \cdot 4\text{H}_2\text{O}$ (1.81 mg L^{-1}), $\text{ZnSO}_4 \cdot 7\text{H}_2\text{O}$ (0.222 mg L^{-1}), $\text{NaMoO}_4 \cdot 2\text{H}_2\text{O}$ (0.39 mg L^{-1}), $\text{CuSO}_4 \cdot 5\text{H}_2\text{O}$ (0.079 mg L^{-1}), $\text{Co}(\text{NO}_3)_2 \cdot 6\text{H}_2\text{O}$ ($49.4 \text{ } \mu\text{g L}^{-1}$)] for 1 week in a bio-shaker (BR-40LF, TAITEC, Tokyo, Japan) agitated at 100 rpm. Pre-culturing was carried out in air at 30 °C under $40 \text{ } \mu\text{mol photons m}^{-2} \text{ s}^{-1}$ illumination by white fluorescent bulbs (Life look HGX; NEC corporation, Tokyo, Japan). Once

the filaments had grown to the mid-exponential phase, they were collected by filtering through a 5- μm pore size polytetrafluoroethylene filter (Millipore, Billerica, MA), washed three times with nitrogen-free BG11 (BG11₀), inoculated into fresh BG11₀ medium at 150 mg dry-cell weight L⁻¹, and grown for 1 week in the BG11₀ medium. After this pre-culturing, those filaments used in our experiment were collected from the flask described above, inoculated into fresh BG11 medium, and grown for 1 week. After that, we took ~10 mL from the culture bottle as a control (0-day filaments). Then, the rest of the filaments in the culture bottle were collected, inoculated into fresh BG11₀ medium, and grown for 15 days. On the fourth, eighth, and fifteenth day after the inoculation, we took ~10 mL from the same culture bottle. Filaments grown in BG11₀ for 4, 8, and 15 days are referred to as 4-, 8-, and 15-day filaments, respectively. The initial optical density at 750 nm (OD₇₅₀) was set to 0.04. *A. variabilis* filaments were at the exponential phase or the stationary phase during 15 days (Fig. 1).

Measurement of steady-state spectra

Steady-state absorption spectra were measured by a spectrometer equipped with an integrating sphere (V-650/ISV-747, JASCO, Tokyo, Japan) at 77 K. Steady-state fluorescence spectra were measured with a spectrofluorometer (FP-6600/PMU-183, JASCO, Tokyo, Japan) at 77 K. The excitation wavelength was 600 nm, which mainly excites PC. For steady-state fluorescence measurements, fluorescence from the surface of sample was monitored at a right angle with respect to the incident light. The steady-state fluorescence spectra were collected using a standard lamp with a known radiation profile.

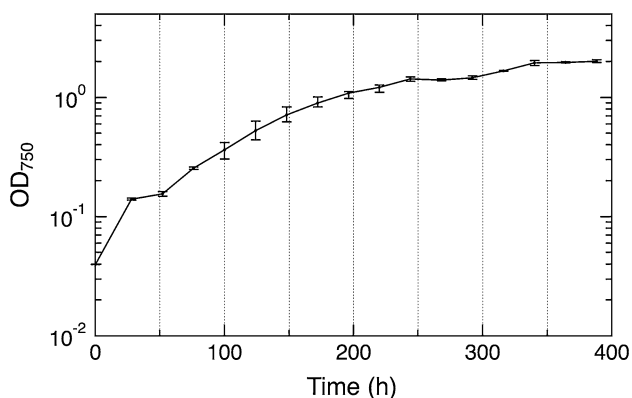


Fig. 1 Growth of *A. variabilis* filaments under nitrogen-depleted condition (BG11₀). Growth was measured as the optical density at 750 nm (OD₇₅₀)

Measurement of time-resolved fluorescence spectra

Time-resolved fluorescence spectra (TRFS) were measured by a time-correlated single photon counting system at 77 K (Akimoto et al. 2012). Excitation was incited by the second harmonic (400 nm) of a Ti: sapphire laser (Tsunami, Spectra-physics, Mountain View, CA, USA) generated by an LBO crystal. This wavelength simultaneously excites all pigments. The time interval for data acquisition was set to 2.4 ps/channel (total time window = 10 ns) or 24.4 ps/channel (100 ns) and the repetition rate of the pulse picker was 2.9 MHz. Therefore, the measurements were unaffected by the excitation pulse up to 100 ns. In this system, the width of the instrumental response function was approximately 40 ps. The fluorescence kinetics were measured at 1-nm intervals (620–770 nm). Fluorescence behaviors were consistent in repeated measurements, confirming constant sample conditions throughout the measurements. Homogenous ice at 77 K was obtained by adding polyethylene glycol (average molecular weight 3,350, final concentration 15 % (w/v), Sigma-Aldrich, USA) to the sample solutions. Prior to experiment, all samples were prepared under dim light. For TRFS measurements, fluorescence from the surface of the sample was monitored as a right angle with respect to the incident light. The TRFS were collected using a substandard lamp with a known profile.

Results

Steady-state absorption and fluorescence spectra

Figure 2 shows the steady-state absorption spectra of *A. variabilis* filaments at 77 K. All absorption spectra were normalized by the Chl Qy absorption band (678 nm). PC peaks twice (at 620 and 632 nm), and the shoulder around 655 nm is assigned to APC. Chl exhibits three absorption peaks at 440, 678, and 710 nm, corresponding to the Chl Soret band, the Chl Qy band, and the lower-energy Chl band of PSI, respectively. The three peaks at 470, 495, and 530 nm are assigned to Car. In the 4-day filaments, the relative intensities of the PBP and Car bands are reduced, but the spectral shape of the Chl Qy band is almost identical in the 4-day and 0-day filaments. The PBP and Chl Qy absorption regions remained largely unchanged throughout the next 4 days. Four notable changes appear in the absorption spectrum of the 15-day filaments; decreased relative intensity of the PBP band, increased relative intensity of the Car band, reduced clarity of the peaks attributed to the Car band, and increased relative intensity of the PSI lower-energy Chl band (Table 1).

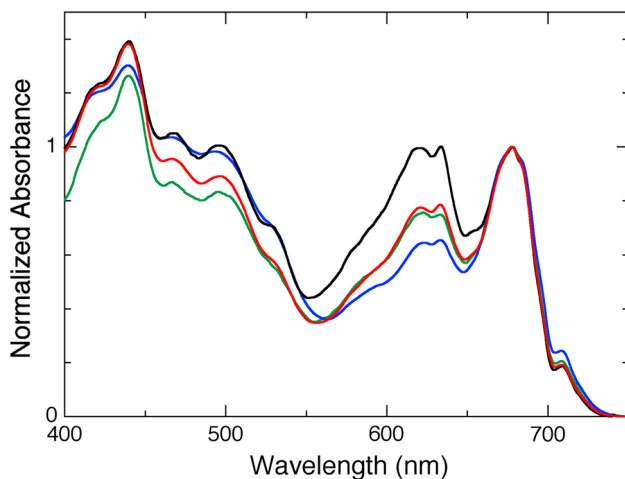


Fig. 2 Steady-state absorption spectra of 0-day (black line), 4-day (red line), 8-day (green line), and 15-day (blue line) filaments grown under nitrogen-poor conditions at 77 K. The spectra are normalized by the Chl Qy band. The values of PC/Chl were obtained after subtracting estimated contribution of the Chl Qy (1,0) band (0.05) from the apparent relative absorbance around 632 nm

Table 1 Intensity ratios in the steady-state absorption spectra (Fig. 2) of *A. variabilis* filaments grown under nitrogen-poor conditions at 77 K

Growth period	Car/Chl	PC/Chl ^a	Chl ₇₁₀ /Chl
0 day	1.0	1.0	1.0
4 day	0.89	0.75	1.0
8 day	0.83	0.74	1.1
15 day	0.98	0.64	1.3

Car carotenoid (495 nm), PC phycocyanin (632 nm), Chl chlorophyll (678 nm), and Chl₇₁₀ lower-energy chlorophyll (710 nm), respectively. Each value is divided by the respective 0-day ratio

^a The values of PC/Chl were obtained after subtracting estimated contribution of the Chl Qy(1,0) band (0.05) from the apparent relative absorbance around 632 nm

Figure 3 shows the steady-state fluorescence spectra of *A. variabilis* filaments at 77 K. All fluorescence spectra were normalized by the PC band (650 nm) (recall that PC is excited by the selected excitation wavelength of 600 nm). The peak at 665 nm is attributed to APC, whereas the two peaks at 685 and 695 nm correspond to PSII red-Chl in CP43 and CP47, respectively (Murata and Satoh 1986), and the peak around 733 nm is associated with PSI red-Chl. The PC/APC fluorescence intensity ratio was lower in the 4-day filaments than in the 0-day filaments, but the PSI/PSII ratio was unchanged. During the fourth to eighth days, the fluorescence intensity of PSII decreased while that of PSI increased. After 15 days of nitrogen depletion, the fluorescence intensity from PSI was greatly increased. The relative intensity of PSII decreased;

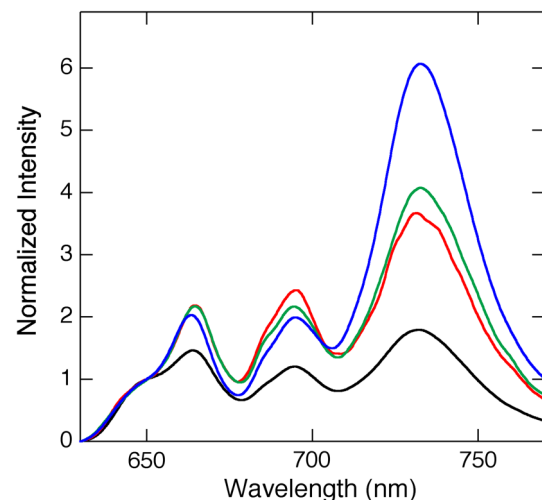


Fig. 3 Steady-state fluorescence spectra of 0-day (black line), 4-day (red line), 8-day (green line), and 15-day (blue line) filaments grown under nitrogen-poor conditions at 77 K. The excitation wavelength (600 nm) selectively excites PC. The spectra are normalized by the PC band

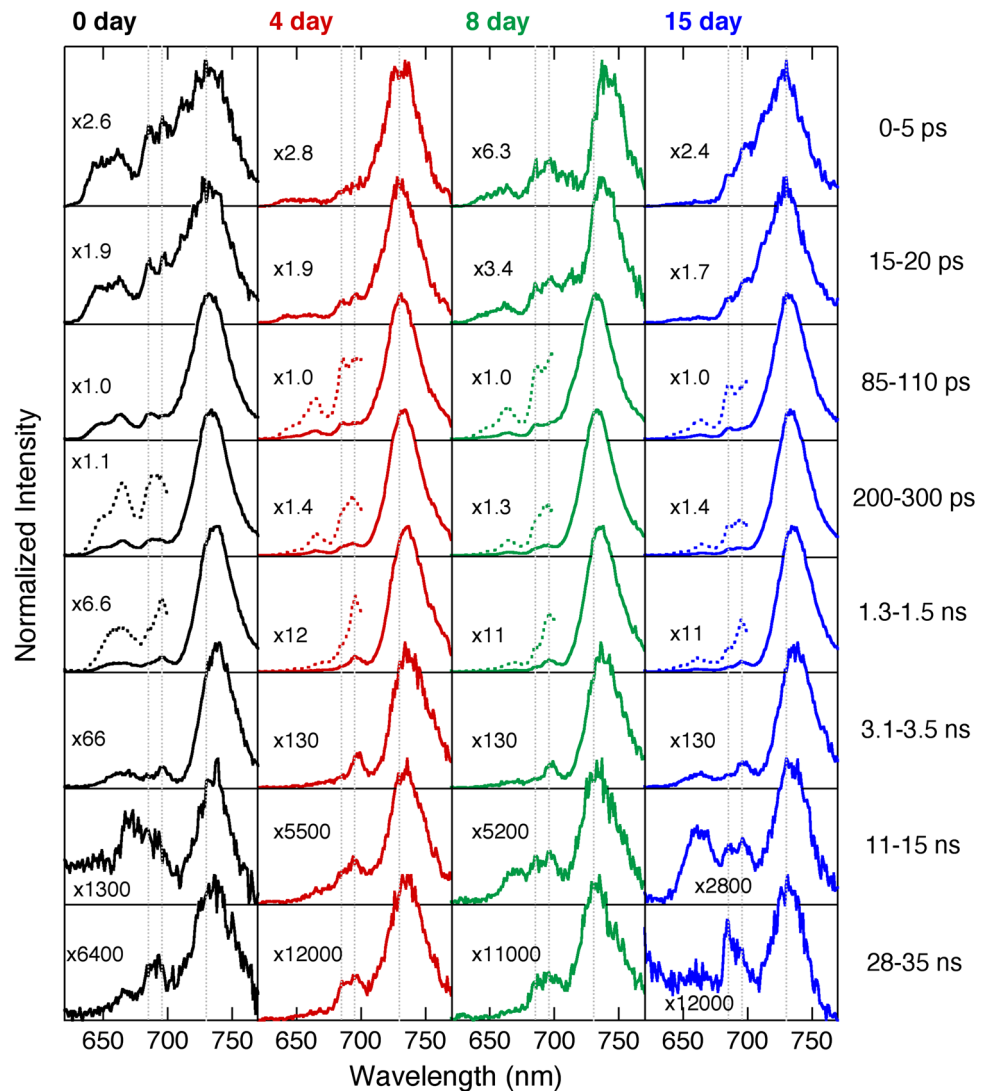
however, peak wavelength remained at 685 and 695 nm, indicating the PSII red-Chls were preserved.

Time-resolved fluorescence spectra and fluorescence decay-associated spectra

Figure 4 shows TRFS of the 0-day, 4-day, 8-day, and 15-day filaments. In the PBP region of the TRFS, the relative fluorescence intensities of PC and APC were reduced under the nitrogen-depleted condition; the PC/PSI ratios of the 0-day, 4-day, 8-day, and 15-day filaments (85–110 ps in Fig. 4) were 10×10^{-2} , 2.2×10^{-2} , 1.6×10^{-2} , and 0.9×10^{-2} , respectively, whereas the respective APC/PSI ratios were 17×10^{-2} , 5.6×10^{-2} , 4.2×10^{-2} , and 2.6×10^{-2} . The PSI peaks immediately following excitation (0–5 ps in Fig. 4) appeared at different wavelengths (733, 734, 740, and 730 nm for the 0-day, 4-day, 8-day, and 15-day filaments, respectively). Note that the fluorescence peaks at a longer wavelength in the 8-day filaments than in the other filaments. On the other hand, after 85 ps, the fluorescence maxima of all samples appear at the same wavelength. In the final TRFS (28–35 ns in Fig. 4), all samples display PSII and PSI peaks, but the spectral shapes of the PSII region differ between the 15-day filaments and the other samples. Specifically, the spectrum of the 15-day filaments features two clear PSII red-Chl bands (at 685 and 695 nm), with the more intense peak appearing at 685 nm. The PSI/PSII ratio increases under the nitrogen-depleted condition (28–35 ns in Fig. 4).

Figure 5 shows the fluorescence decay-associated spectra (FDAS). The fluorescence curves were fitted by sums of exponentials with common lifetimes as follows:

Fig. 4 Time-resolved fluorescence spectra of 0-day (black line), 4-day (red line), 8-day (green line), and 15-day (blue line) filaments grown under nitrogen-poor conditions at 77 K. The spectra are normalized by the PSI red-Chl band. Dotted lines show $\times 5$ magnifications of the spectra. Numbers shown on individual spectra indicate magnification factors relative to that of the most intense spectrum. The gray vertical lines indicate 685, 695, and 730 nm from left to right

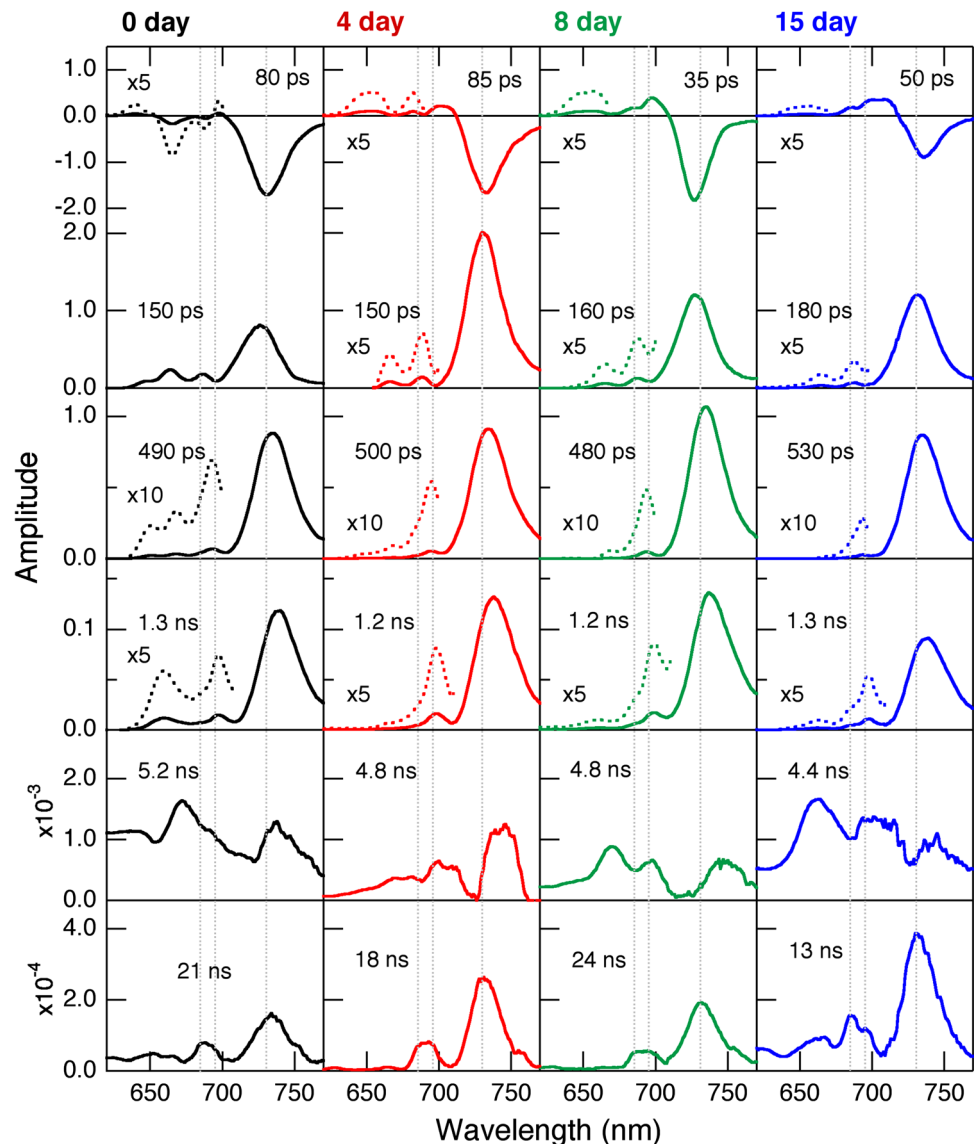


$$F(t, \lambda) = \sum_{n=1}^6 A_n(\lambda) \exp\left(-\frac{t}{\tau_n}\right).$$

Positive and negative amplitudes $A_n(\lambda)$ indicate fluorescence decay and rise over time, respectively. Therefore, a positive and negative pair of amplitudes indicates that energy is transferred from a pigment with positive amplitude to one with negative amplitude (Akimoto et al. 2012). The peak around 665 nm (APC) in the PBS region of the first FDAS (80 ps) has a negative amplitude at day 0, but establishes a positive amplitude at later growth times. In the PBS region of the second, third, and fourth FDAS, the PC and APC contributions reduce under the nitrogen-depleted condition. In the Chl region of the first FDAS, the 8-day filaments exhibit a negative peak at shorter wavelength (727 nm) than the other filaments (731–736 nm). In the second FDAS, the fluorescence peak wavelengths depend on the growth period, reflecting PSI red-Chls of

different energies (F726, F730, F728, F732). The fluorescence maxima coincide in the third and fourth FDAS, indicating that the PSI red-Chls in all samples possessed very similar energies (F735 and F738 in the third and fourth FDAS, respectively). The long-lived fluorescences are revealed in the sixth FDAS (13–24 ns). Following charge recombination between the special pair (P680) and pheophytin *a* in the PSII reaction center, an excited state is re-generated and delayed fluorescence is emitted. The time constant of this fluorescence exceeds the lifetime of an isolated Chl (Mimuro et al. 2007). From the delayed fluorescence spectra, we can understand the interaction between PSI and PSII (Yokono et al. 2011). The relative PSI/PSII ratios of the 0-day, 4-day, and 8-day filaments in the sixth FDAS were 1.0, 1.4, and 1.5, respectively, suggesting that the relative amount of PSII interacting with PSI increased compared with the amount of free PSII under the nitrogen-depleted condition. In addition, the time

Fig. 5 Fluorescence decay-associated spectra of 0-day (black line), 4-day (red line), 8-day (green line), and 15-day (blue line) filaments at 77 K grown under nitrogen-poor conditions. Dotted lines show $\times 5$ or $\times 10$ magnifications of the spectra. The gray vertical lines indicate 685, 695, and 730 nm from left to right



constant of charge recombination was shortest for the 15-day filaments and the spectral shape differed between the 15-day filaments and the other samples. The lifetimes of 4–5 ns (the fifth FDAS) might be assignable to fluorescences from free pigments.

Discussion

Energy transfer process within PBS

In the steady-state absorption spectra (Fig. 2), the relative PC intensities in filaments deprived of nitrogen gradually decreased over the growth period, reflecting the PC degradation. Specifically, the PC band intensities (relative to the Chl Qy band) in the 4-day, 8-day, and 15-day filaments

reduced to 75, 74, and 64 % of the initial value (0-day filaments), respectively (see Table 1). PC degradation has also been reported in nitrogen-depleted *A. nidulans* and *A. platensis* (Allen and Smith 1969; Peter et al. 2010). On the other hand, the intensities of the APC/PC fluorescence ratios increased under the nitrogen-depleted condition (Table 2), but in a non-straightforward manner (Fig. 3). Inconsistent with the absorption changes, the APC/PC decrease in the 15-day filaments was preceded by an increase in the 4-day and 8-day filaments. In the first FDAS (the 80-ps component, Fig. 4), PC–APC energy transfer manifested as a positive–negative amplitude pair (in the 0-day filaments, the positive and negative amplitudes appeared around 640 nm (PC) and 665 nm (APC), respectively). However, in the 4-day, 8-day, and 15-day filaments, all amplitudes around 665 nm were positive (the

Table 2 Fluorescence intensity ratios in the steady-state fluorescence (SF) spectra of *A. variabilis* filaments grown under nitrogen-poor conditions at 77 K (Fig. 3), and those in the delayed fluorescence (DF) spectra (Fig. 5)

Growth period	SF				DF
	APC/PC	PSII/PC	PSI/PC	PSI/PSII	PSI/PSII
0 day	1.0	1.0	1.0	1.0	1.0
4 day	1.5	2.0	2.1	1.0	1.4
8 day	1.5	1.8	2.3	1.3	1.5
15 day	1.4	1.7	3.4	2.1	1.3

PC phycocyanin (650 nm), APC allophycocyanin (665 nm), PSII photosystem II (695 nm), and PSI photosystem I (733 nm), respectively. Each value is divided by the respective 0-day ratio

35–85 ps components). APC is excited by two mechanisms; direct excitation by the laser pulse and acquisition of energy from PC. Therefore, the positive amplitudes in the spectra of 4-day, 8-day, and 15-day filaments probably reflect direct excitation of APC by the laser pulse, which would increasingly surpass energy acquisition from PC as the PC (energy donor) degraded. This phenomenon might explain the dynamics of the APC/PC ratio under the nitrogen-depleted condition. Among the first and second FDAS (the 35–85 and 150–180 ps components) of the 4-day, 8-day, and 15-day filaments, the APC amplitude was smallest in the 15-day filaments (Fig. 5), indicating that less APC was involved in energy transfer in the 15-day filaments.

Energy transfer process from PSII to PSI

Because charge recombination occurs only at the PSII reaction center at 77 K and requires tens of nanoseconds (Mimuro et al. 2007), the PSI/PSII ratio in the delayed fluorescence spectrum reflects the contribution of the PSII → PSI energy transfer (i.e. spillover). Excitation energy transfer from PSII to PSI raises the PSI/PSII ratio (Yokono et al. 2011). Therefore, the higher the PSI/PSII ratio, the larger the amount of PSII interacting with PSI (PSI–PSII supercomplex) and the smaller the amount of free PSII (PSII complex). In the sixth FDAS, the relative PSI/PSII ratios of the 0-day, 4-day, 8-day, and 15-day filaments were 1.0, 1.4, 1.5, and 1.3, respectively. The increasing PSI/PSII ratios in the 4-day, 8-day, and 15-day filaments indicate that more PSI–PSII supercomplex forms in a nitrogen-depleted environment. The increased contribution of the PSI–PSII supercomplex can be explained by two phenomena; degradation of PSII complexes under nitrogen-depleted conditions, and preferential formation of PSI–PSII supercomplexes under nitrogen-depleted conditions. The relative intensity of the 710-nm band increased in the absorption spectra of the 15-day filaments (Fig. 2),

indicating that the relative PSI content increased under the nitrogen-depleted condition. Therefore, the more probable cause of the increased PSI/PSII ratio in the delayed fluorescence is decrease in the amount of the free PSII.

Energy transfer process from PBS to PSI

PBS transfers excitation energy to PSI as well as to PSII (Mullineaux 2008). Energy is transferred from PBS to PSI via two pathways; direct energy transfer from PBS to PSI (the PBS → PSI energy transfer) (Mullineaux 1992) and energy transfer from PBS to PSI via PSII (PBS → PSII → PSI energy transfer) (Butler and Kitajima 1975; Bruce et al. 1985). Note that the former transfer is independent of the PSII → PSI energy transfer, whereas the latter depends on the PSII → PSI energy transfer. Therefore, if the PBS → PSII → PSI energy transfer is the only pathway (lack of the direct transfer), the PSI/PSII ratios in the steady-state and delayed fluorescences should be identical. In the steady-state fluorescence spectra (Fig. 3), the PSI/PSII ratio began changing after 4 days of nitrogen depletion, and had doubled in the 15-day filaments (Table 2). On the other hand, in the delayed fluorescence spectra, the PSI/PSII ratio changed during the initial 4 days of growth, and remained stable throughout the next 11 days (Table 2). These behaviors suggest that both PBS → PSII → PSI and PBS → PSI energy transfers contributed to the PBS–PSI energy transfer, especially after 8 days of nitrogen depletion.

Energy transfer in PSI red-Chls

The PSI monomer contains 9–11 red-Chls with slightly different energies (Jordan et al. 2001). At 77 K, excitation energy is transferred from higher-energy PSI red-Chl to lower-energy ones. In the second FDAS (Fig. 5), the peak wavelength in the PSI fluorescence region depended on the growth period, being 726, 730, 728, and 731 nm in the 0-day, 4-day, 8-day, and 15-day filaments, respectively. The third and fourth FDAS of all filaments exhibited peaks at 735 nm (F735) and 738 nm (F738), respectively (Fig. 5). These behaviors suggest that the initial excitation–relaxation process involving PSI red-Chls altered throughout the growth, but that relaxation stabilized once energy had been transferred to F735. The negative peak in the first FDAS appeared at 731, 732, 727, and 735 nm in the 0-day, 4-day, 8-day, and 15-day filaments, respectively, showing a blue shift during the first 8 days, followed by a red shift (Fig. 5). Therefore, throughout the growth period, different PSI red-Chls took the energy acceptor role. After the first 8 days, more of the energy transfer to PSI was contributed by PBS → PSI transfer; before this time, the energy transfer was largely contributed by PSII → PSI transfer (Table 2). Hence, the

blue and red shifts correspond to increased contributions of the PSII → PSI and PBS → PSI energy transfers, respectively. It appears that the high-energy red-Chls play the acceptor role during PSII → PSI energy transfer, while their lower-energy counterparts take this role during PBS → PSI energy transfer. To determine the binding sites and precise routes of the PBS → PSI and PSII → PSI energy transfers, we must assign locations to the PSI red-Chls.

Excitation relaxation within PSII

When the PSII reaction center combines with the core antenna complexes, the delayed fluorescence exhibits two PSII red-Chl bands at 685 and 695 nm (Yokono et al. 2012), coming from CP43 and CP47, respectively (Murata and Satoh 1986). The PSII fluorescence in the sixth FDAS of the 15-day filaments differed from those of the other filaments; specifically, the amplitude was higher at 685 nm than at 695 nm in this spectrum (Fig. 5). Strong interaction between the monomer units of the PSII dimer triggers excitation energy transfer from CP43 to its neighboring CP47; if the dimers weakly interact, no transfer occurs (Yokono et al. 2012). Therefore, the intense 685-nm band in the delayed fluorescence of the 15-day filaments indicates that long-term nitrogen deprivation weakened the PSII dimer interaction in the *Anabaena* filaments. The time constants of the delayed fluorescence in the 0-day, 4-day, 8-day, and 15-day filaments were 21, 18, 24, and 13 ns, respectively (Fig. 5). The shortened time constant in the 15-day filaments suggests that nitrogen depletion also affects the charge recombination process.

Changes in the Car absorption

According to previous studies (Allen and Smith 1969), the Car content (relative to Chl *a*) increases in *A. nidulans* exposed to nitrogen limitation for 10–14 days. The major Cars of *A. nidulans* are β -carotene (33 %), zeaxanthin (49 %), and caloxanthin (13 %) (Takaichi et al. 2005). Nitrogen depletion also affects the Car composition, inducing gradual decline of β -carotene and increases of zeaxanthin and caloxanthin in nitrogen-deprived *A. nidulans* (Gombos and Vigh 1986). On the other hand, in the present absorption spectra of *A. variabilis* filaments (see Fig. 2), the relative intensities of Cars decreased in the 4-day and 8-day filaments and recovered in the 15-day filaments. The vibrational structure of Car absorption was clearly recognizable throughout the first 8 days of growth, but the peaks became unclear throughout the next 7 days. This indicates that, although the relative intensities of Car absorption were almost identical in the 0-day and 15-day

filaments, the Car compositions were different. The major Cars of *A. variabilis* are β -carotene (51 %), echinenone (20 %), and canthaxanthin (22 %) (Takaichi et al. 2006). The latter two absorb at longer wavelengths than β -carotene. Therefore, the changing Car absorption throughout the growth may be explained by reduction in the relative amount of β -carotene during the initial 8 days, followed by increased relative amount of other Cars. X-ray crystal structures of PSII and PSI have revealed Chl *a*-to- β -carotene ratios of 35:11 in the PSII monomer (Umena et al. 2011) and 96:22 in the PSI monomer (Jordan et al. 2001). Based on these results, the β -carotene/Chl *a* ratios in PSII and PSI are 0.31 and 0.23, respectively. Clearly, PSII contains more β -carotenes than PSI, and the β -carotene/Chl *a* ratio will reduce with decreasing relative amount of PSII to PSI in whole filaments. Therefore, PSII degradation can reasonably explain, at least partly, the decrease in relative Car content throughout the initial 8 days.

The time constants of the second to fourth FDAS remained fairly constant throughout the growth period, suggesting that the altered Car content and composition did not affect the excitation–relaxation occurring on the 100 ps to ns time scales. Therefore, the additional Cars found in the 15-day filaments are unlikely to work as quenchers in PSs.

Summary

Using steady-state and time-resolved spectroscopies, we investigated the energy transfer dynamics in intact *A. variabilis* filaments throughout 15 days of nitrogen depletion. Nitrogen depletion induced modifications of the pigment composition and altered the energy transfer processes. As time passed, the relative amount of PC monotonically decreased, whereas the relative Car content initially decreased and then increased, with formation of lower-energy Car(s). Nitrogen depletion induced the following changes in the energy transfer processes: (1) decreased relative amount of PC related to PC → APC energy transfer, (2) facilitation of PSII → PSI energy transfer and suppression of PBS → PSI energy transfer, (3) regarding PBS–PSI energy transfer, high contribution of PSII → PSI transfer during the first 4 days, followed by increased contribution of direct PBS → PSI transfer after the 8th day, (4) suppression of energy transfer within the PSII dimer after long-term growth, and (5) appearance of additional Cars in the 15-day filaments, which are unlikely to work as quenchers in the PSs. Nitrogen depletion also affected the charge recombination at the PSII reaction center. To further understand the energy transfer dynamics of nitrogen-deprived *Anabaena*, we must conduct further

energy transfer studies in vegetative cells, heterocysts, and isolated pigment–protein complexes.

Acknowledgments The authors thank Prof. M. Ikeuchi and Dr. M. Watanabe for providing technical information about the culturing procedure. This work was supported in part by a Grant-in-Aid for Scientific Research from JSPS (No. 23370013) to S. Akimoto.

References

- Akimoto S, Yokono M, Hamada F, Teshigahara A, Aikawa S, Kondo A (2012) Adaptation of light-harvesting systems of *Arthrospira platensis* to light conditions, probed by time-resolved fluorescence spectroscopy. *Biochim Biophys Acta* 1817:1483–1489
- Akimoto S, Yokono M, Aikawa S, Kondo A (2013) Modification of energy-transfer processes in the cyanobacterium, *Arthrospira platensis*, to adapt to light conditions, probed by time-resolved fluorescence spectroscopy. *Photosynth Res* 117:235–243
- Allen MM, Smith AJ (1969) Nitrogen chlorosis in blue-green algae. *Arch Microbiol* 69:114–120
- Bruce D, Biggins J, Steiner T, Thewalt M (1985) Mechanism of the light state transition in photosynthesis—IV. Picosecond fluorescence spectroscopy of *Anacystis nidulans* and *Porphyridium cruentum* in state 1 and state 2 at 77 K. *Biochim Biophys Acta* 806:237–246
- Butler WL, Kitajima M (1975) Energy transfer between photosystem II and photosystem I in chloroplasts. *Biochim Biophys Acta* 396:72–85
- Collier JL, Herbert SK, Fork DC, Grossman AR (1994) Changes in the cyanobacterial photosynthetic apparatus during acclimation to macronutrient deprivation. *Photosynth Res* 42:173–183
- Flores E, Herrero A (2010) Compartmentalized function through cell differentiation in filamentous cyanobacteria. *Nat Rev Microbiol* 8:39–50
- Ghosh AK, Govindjee (1966) Transfer of the excitation energy in *Anacystis nidulans* grown to obtain different pigment ratios. *Biophys J* 6:611–619
- Golden JW, Yoon HS (2003) Heterocyst development in *Anabaena*. *Curr Opin Microbiol* 6:557–563
- Gombos Z, Vigh L (1986) Primary role of the cytoplasmic membrane in thermal acclimation evidenced in nitrate-starved cells of the blue-green alga, *Anacystis nidulans*. *Plant Physiol* 80:415–419
- Haselkorn R (1978) Heterocysts. *Ann Rev Plant Physiol* 29:319–344
- Jensen TE, Rachlin JW (1984) Effect of varying sulphur deficiency on structural components of a cyanobacterium *Synechococcus leopoliensis*: a morphometric study. *Cytobios* 41:35–46
- Jordan P, Fromme P, Witt HT, Klukas O, Saenger W, Krauß N (2001) Three-dimensional structure of cyanobacterial photosystem I at 2.5 Å resolution. *Nature* 411:909–917
- Kumazaki S, Akari M, Hasegawa M (2013) Transformation of thylakoids membranes during differentiation from vegetative cell into heterocyst visualized by microscopic spectral imaging. *Plant Physiol* 161:1321–1333
- Lau RH, Mackenzie MM, Doolittle WF (1977) Phycocyanin synthesis and degradation in the blue-green bacterium *Anacystis nidulans*. *J Bacteriol* 132:771–778
- Melis A (1999) Photosystem-II damage and repair cycle in chloroplasts: what modulates the rate of photodamage in vivo? *Trends Plant Sci* 4:130–135
- Mimuro M, Akimoto S, Tomo T, Yokono M, Miyashita H, Tsuchiya T (2007) Delayed fluorescence observed in the nanosecond time region at 77 K originates directly from the photosystem II reaction center. *Biochim Biophys Acta* 1767:327–334
- Mullineaux CW (1992) Excitation energy transfer from phycobilisomes to photosystem I in a cyanobacterium. *Biochim Biophys Acta* 1100:285–292
- Mullineaux CW (2008) Phycobilisome-reaction centre interaction in cyanobacteria. *Photosynth Res* 95:175–182
- Murata N, Satoh K (1986) Absorption and fluorescence emission by intact cells, chloroplasts, and chlorophyll–protein complexes. In: Govindjee, Ames J, Fork DC (eds) *Light emission by plants and bacteria*. Academic Press, Orlando, pp 137–159
- Owens TG (1996) Processing of excitation energy by antenna pigments. In: Baker NR (ed) *Photosynthesis and the environment*. Kluwer Academic Publishers, Dordrecht, pp 1–23
- Peter P, Sarma AP, Hasan MDA, Murthy SDS (2010) Studies on the impact of nitrogen starvation on the photosynthetic pigments through spectral properties of the cyanobacterium, *Spirulina platensis*: identification of target phycobiliprotein under nitrogen chlorosis. *Bot Res Int* 3:30–34
- Sugiura K, Itoh S (2012) Single-cell confocal spectrometry of a filamentous cyanobacterium *Nostoc* at room and cryogenic temperature. Diversity and differentiation of pigment systems in 311 cells. *Plant Cell Physiol* 53:1492–1506
- Takahashi S, Badger MR (2011) Photoprotection in plants: a new light on photosystem II damage. *Trends Plant Sci* 16:53–60
- Takaichi S, Mochimaru M, Maoka T, Katoh H (2005) Myxol and 4-ketomyxol 2'-fucosides, not rhamnosides, from *Anabaena* sp. PCC 7120 and *Nostoc punctiforme* PCC 73102, and proposal for the biosynthetic pathway of carotenoids. *Plant Cell Physiol* 46:497–504
- Takaichi S, Mochimaru M, Maoka T (2006) Presence of free myxol and 4-hydroxymyxol and absence of myxol glycosides in *Anabaena variabilis* ATCC 29413, and proposal of a biosynthetic pathway of carotenoids. *Plant Cell Physiol* 47:211–216
- Umena Y, Kawakami K, Shen JR, Kamiya N (2011) Crystal structure of oxygen-evolving photosystem II at a resolution of 1.9 Å. *Nature* 473:55–61
- Watanabe M, Ikeuchi M (2013) Phycobilisome: architecture of a light-harvesting supercomplex. *Photosynth Res* 116:265–276
- Watanabe M, Semchonok D, Webber-Birungi MT, Ehira S, Kondo K, Narikawa R, Ohmori M, Boekema EJ, Ikeuchi M (2014) Attachment of phycobilisomes in an antenna-photosystem I supercomplex of cyanobacteria. *PNAS* 111:2512–2517
- Yokono M, Murakami A, Akimoto S (2011) Excitation energy transfer between photosystem II and photosystem I in red algae: larger amounts of phycobilisome enhance spillover. *Biochim Biophys Acta* 1807:847–853
- Yokono M, Tomo T, Nagao R, Ito H, Tanaka A, Akimoto S (2012) Alterations in photosynthetic pigments and amino acid composition of D1 protein change energy distribution in photosystem II. *Biochim Biophys Acta* 1817:754–759
- Zhao J, Zhao J, Zhang J, Jiang L (1999) Phycobilisome from *Anabaena variabilis* Kütz. and its model conjugates. *Photosynthetica* 36:163–170